

Analyst

Accepted Manuscript



This is an *Accepted Manuscript*, which has been through the Royal Society of Chemistry peer review process and has been accepted for publication.

Accepted Manuscripts are published online shortly after acceptance, before technical editing, formatting and proof reading. Using this free service, authors can make their results available to the community, in citable form, before we publish the edited article. We will replace this *Accepted Manuscript* with the edited and formatted *Advance Article* as soon as it is available.

You can find more information about *Accepted Manuscripts* in the [Information for Authors](#).

Please note that technical editing may introduce minor changes to the text and/or graphics, which may alter content. The journal's standard [Terms & Conditions](#) and the [Ethical guidelines](#) still apply. In no event shall the Royal Society of Chemistry be held responsible for any errors or omissions in this *Accepted Manuscript* or any consequences arising from the use of any information it contains.

Cite this: DOI: 10.1039/c0xx00000x

www.rsc.org/xxxxxx

ARTICLE TYPE

Double enzymatic cascade reactions within FeSe-Pt@SiO₂ nanospheres: synthesis and application toward colorimetric biosensing of H₂O₂ and glucose

Fengmin Qiao, Zhenzhen Wang, Ke Xu, Shiyun Ai*

Received (in XXX, XXX) Xth XXXXXXXXX 20XX, Accepted Xth XXXXXXXXX 20XX

DOI: 10.1039/b000000x

A facile process was developed for the synthesis of FeSe-Pt@SiO₂ nanospheres based on the hydrothermal treatment FeCl₃·6H₂O, selenium and NaBH₄ in ethanolamine solvent, followed by reducing HPtCl₄ with NaBH₄ in the presence of FeSe particles to obtain FeSe coated with Pt NPs (FeSe-Pt), ending with a surfactant assembled sol-gel process to obtain FeSe-Pt@SiO₂. The morphology and composition of FeSe-Pt@SiO₂ were characterized by transmission electron microscopy, high resolution TEM, X-ray diffraction and fourier transform infrared spectra. Structural analyses revealed that FeSe-Pt@SiO₂ were composed of regular spherical with smooth surfaces due to the SiO₂ shells, compared with FeSe particles with 150 nm lateral diameter. The prepared FeSe-Pt@SiO₂ nanospheres possessed both intrinsic glucose oxidase (GOx-) and peroxidase-mimic activities, and engineered an artificial enzymatic cascade system with high activity and stability based on this nanostructure. The good catalytic performance of the composites could be attributed to the synergy between the functions of FeSe particles and Pt NPs. Significantly, the FeSe-Pt@SiO₂ nanospheres as robust nanoreactors can catalyze a self-organized cascade reaction, which includes oxidation of glucose by oxygen to yield gluconic acid and H₂O₂, and then oxidation of 3,3',5,5'-tetramethylbenzidine (TMB) by H₂O₂ to produce a colour change. Colorimetric detections of H₂O₂ and glucose using the FeSe-Pt@SiO₂ nanospheres were conducted with high detection sensitivities, 0.227 nM and 1.136 nM, respectively, demonstrating the feasibility of practical sensing applications. It is therefore believed that our findings in this study could open up the possibility of utilizing FeSe-Pt@SiO₂ nanospheres as enzymatic mimics in diagnostics and biotechnology fields.

1 Introduction

Cascade reactions, typically defined as a consecutive series of chemical reactions proceeding in a concurrent fashion, have attracted scientists' attention in recent years. Generally, this typology of reaction can be classified into domino, one-pot, or tandem reactions, and the intrinsic advantages correlated to these types of consecutive reactions are clear: step-saving, atom economy, therefore, high yield and efficiency of the chemical process^{1,2}. Enzymatic conversions of cascade reactions are often catalyzed by multienzyme complexes which are prevalent nanomachines in nature^{3,4}. Among these natural multienzymes, cascade enzymes, each dedicated to a single catalytic activity in sequential chemical conversions, have attracted sustained attention⁵⁻⁷. Natural multienzymes, however, also suffer from some intrinsic drawbacks such as sensitivity of catalytic activity to environmental conditions and relatively low stability (denaturation and digestion). In addition, high costs in preparation and purification also limit their large scale applications^{8,9}. Intrigued by nature's design of multienzyme

architectures, chemists and metabolic engineers construct artificial multienzyme complexes by harnessing specific and noncovalent biorecognitions.

During the past decade, nanostructured materials (specially the active nanoparticles (NPs) and biomaterials (as remarkable heterogeneous catalysts for different organic reactions) has undergone explosive growth, thanks to the development of more efficient synthetic methodologies^{10,11}. Biocatalysts can be integrated in synthetic processes in combination with chemical processes or in cascade reactions in which a series of enzymes catalyze successive synthetic steps¹²⁻¹⁴. For example, cascade enzymes have been assembled on artificial scaffolding or synthetic scaffold proteins through protein-protein interactions¹⁵, on DNA templates through protein-DNA interactions¹⁶, on chemical scaffolds through bioconjugation reactions, or alternatively, enzyme proximity has been realized by physical compartmentalization¹⁷. Artificial self-assembled nanodevices have also been developed to mimic key biofunctions, and various nucleic acid-based functional nanoassemblies have been reported¹⁸. However, combining protein, nucleic acid and lipid

alone is not sufficient to form a functional cell. One desirable but challenging topic is the assembly of various nanomaterials together into ordered functional systems, a common phenomenon in nature, but much more difficult to achieve with artificial components.

In recent years, core-shell structured materials with a void space between the core and the shell have been intensively studied. The void space within the shell provides a unique confined space for the core material in confined catalysis, drug release, lithium-ion batteries, etc^{19, 20}. The core-shell structured material can be regarded as a nanoreactor for catalytic reactions^{21, 22}. Several reports have shown that core-shell structured material with noble metal inside the shell had high catalytic activities in several important reactions, including reduction of nitrophenol, oxidation of aerobic alcohol, Suzuki reaction, etc²³⁻²⁵. Very recently, metal nanomaterials have been explored to mimic the functions of natural enzymes²⁶⁻²⁸. Pt NPs with different surface modifications have been found to exhibit multienzyme mimetic properties^{29, 30}. However, the potential of Pt NPs as enzyme mimics is limited by their relatively low catalytic activities and stability. Recently, the emergence and recent advance of nanotechnology opens new opportunities for the development of nanoparticles with stable and high catalytic activity³¹⁻³³. Most of the chemical applications of metallic NPs in catalysis are based on their use as simple NPs or supported on inorganic materials^{34, 35}. The possibility to immobilize the NPs by these strategies generates heterogeneous nanocatalysts with better performance. For example, gum acacia (GA), a highly branched neutral or slightly acidic arabinogalactan polysaccharide, has been used as a support to deposit palladium NPs. This strategy permits access to heterogeneous Pd catalysts, where the small NPs are generated *in situ* by the polymer, which acts in reducing and stabilizing the metal³⁶. Especially, magnetic nanoparticles (MNPs), which are in general considered to be chemically and biologically inert, have attracted much interest because of their interesting biomedical applications such as protein immobilization and separation, magnetic targeting, biosensor, and drug delivery, tissue engineering^{37, 38}, mediator of cancer therapy³⁹ and so on. In particular, magnetite (Fe₃O₄) has been widely used as an artificial peroxidase and can effectively catalyze the reduction of H₂O₂ and therefore, MNPs have been investigated more and more as peroxidase enzyme mimetics^{31, 40}.

Herein, we report novel, discrete and monodisperse FeSe-Pt@SiO₂ nanospheres with both high GOx and peroxidase-mimic activities. On the surface of FeSe cores, ultrafine Pt NPs with high GOx-mimic catalytic activity are dispersed. Furthermore, FeSe-Pt particles are encapsulated in SiO₂ shells to hinder the aggregation and keep them stable even under harsh conditions. Based on these functional units, the FeSe-Pt@SiO₂ nanospheres as robust nanoreactors can catalyze a self-organized cascade reaction, which includes oxidation of glucose by oxygen to yield gluconic acid and H₂O₂, and then oxidation of 3,3,5,5-tetramethylbenzidine (TMB) by H₂O₂ to produce a colour change. What is more, we show that both glucose oxidase- and peroxidase-mimic activities are combined in one nanoparticle to simulate the enzymatic cascade system without the help of natural enzymes.

2 Experimental section

2.1 Reagents

Ferric chloride hexahydrate (FeCl₃·6H₂O), selenium (Se), ethanol amine, tetraethyl orthosilicate (TEOS), cetyltrimethylammonium bromide (CTAB), H₂PtCl₄·4H₂O (1.62%), H₂O₂, ammonia solution (28%), sodium acetate (NaAc), acetic acid, ethanol and NaBH₄ were of analytical grade and purchased from Aladdin (Shanghai, China). Hydrogen peroxide (H₂O₂), glucose and 3,3,5,5-tetramethylbenzidine (TMB) were obtained from Sigma-Aldrich. Acetate buffer solution (100 mM, pH from 2.0 to 9.0) were used in this work and double distilled deionized water was applied throughout the experiment. All chemicals used in this work were of analytical grade and used as received without further purification. Serum samples were obtained from Hospital of Shandong Agricultural University.

The morphologies and crystal structures of the products observed by transmission electron microscopy (TEM) and high-resolution TEM (HRTEM) using a JEM-2010 TEM. The crystal phase was investigated by a Rigaku DLMAX-2550 V diffractometer (40 kV, Cu K_α (λ= 1.54056 Å), 2θ range 5-80°, scan speed of 6°/min). Fourier transform infrared (FT-IR) spectra were obtained on a Thermo Nicolet-380 IR spectrophotometer (USA). Kinetic measurements and UV-Vis absorption spectra were carried out on a UV-2450 Shimadzu Vis-spectrometer (Japan).

2.2 Synthesis of FeSe-Pt particles

FeSe particles were obtained via a hydrothermal method. Typically, 0.600 g FeCl₃·6H₂O, 0.237 g selenium and 0.539 g NaBH₄ were first dissolved in 54 mL ethanol amine with stirring until the mixture was uniform. The obtained solution was sealed in an 60 mL autoclave. The autoclave was heated at 180 °C for 24 h, and then allowed to cool to room temperature. The products were washed with ethanol and water for several times, dried at 60 °C under vacuum for 4 h, and collected for further study. 40 mg prepared FeSe particles were dispersed in 50 mL nitrogen-saturated water by sonication for 5 min. Subsequently, 0.5 mL of H₂PtCl₄·4H₂O (1.62%) solution was added to above dispersion, and then mechanically stirred for 30 min. A freshly prepared NaBH₄ (2 mL; 0.15 M) was added into the above mixture under vigorous stirring. After the resulted suspension was stirred for another 30 min, the solution containing FeSe-Pt particles was obtained. With the help of a magnet, the microspheres were separated, and washed with nitrogen-saturated water for 3 times.

2.3 Synthesis of FeSe-Pt@SiO₂ microspheres

To enhance the stability of the obtained FeSe-Pt particles, a mesoporous silica shell was introduced according a reported method^{41, 42}. FeSe-Pt particles (100 mg) were added into a mixed solution containing CTAB (40 mg), deionized water (25 mL), concentrated ammonia solution (0.5 mL), and ethanol (37 mL). After the mixed solution was ultrasonicated for 20 min, 120 μL of TEOS was added dropwise to the dispersion under vigorous stirring. After continuous stirring for 8h at room temperature, the product was washed with ethanol and water for several times, dried at 60 °C under vacuum for 4 h, and collected for further study, and FeSe-Pt@SiO₂ composite microspheres were obtained.

2.4 Peroxidase-mimic activity and construction of the artificial enzymatic cascade system

Firstly, we investigated the peroxidase-mimic activity of FeSe-Pt@SiO₂ nanospheres. The peroxidase-mimic catalytic reactions were carried out at room temperature in a 500 μ L reaction system containing acetate buffer solution (100 mM, pH 4.0) with FeSe-Pt@SiO₂ nanospheres (30 μ g mL⁻¹) in the presence of 1.44 mM H₂O₂, using 115 μ M TMB as the substrate.

The construction of the artificial enzymatic cascade system was performed as above experiment using glucose instead of H₂O₂. Firstly, FeSe-Pt@SiO₂ nanospheres (30 μ g mL⁻¹) and glucose (2.88 mM) dissolved in 100 mM acetate buffer solution (pH 4.0, air saturated) were mixed and incubated at room temperature for 1h; then 115 μ M TMB were added to the above reaction solution. The final solution was used for kinetic studies.

As the amount of enzyme mimic has a serious effect on the results, we strictly controlled the amount of FeSe-Pt@SiO₂ nanospheres in the catalytic reactions and the measurements were carried out by varying concentrations of FeSe-Pt@SiO₂ nanospheres catalysts (3-30 μ g mL⁻¹), the H₂O₂ (0-9.0 mM), the buffer solution pH value (2.0-9.0) in 100 mM acetate buffer and the temperature ranging from 0 to 55 $^{\circ}$ C.

2.5 Biosensing

H₂O₂ detection was realized as follows. Firstly, 90 μ L of 115 μ M TMB, 20 μ L of 30 μ g mL⁻¹ FeSe-Pt@SiO₂, and 90 μ L of H₂O₂ with different concentrations were added into 300 μ L of 100 mM acetate buffer (pH 4.0). Then, the mixed solution was used for adsorption spectroscopy measurement with the time-drive method.

Glucose detection was performed in air saturated solution as reported previously: Firstly, FeSe-Pt@SiO₂ nanospheres (30 μ g mL⁻¹) and glucose with different concentrations dissolved in 100 mM acetate buffer solution (pH 4.0, air saturated) were mixed and incubated at room temperature for 1h; then 115 μ M TMB were added to the above reaction solution. The final solution was used for kinetic studies.

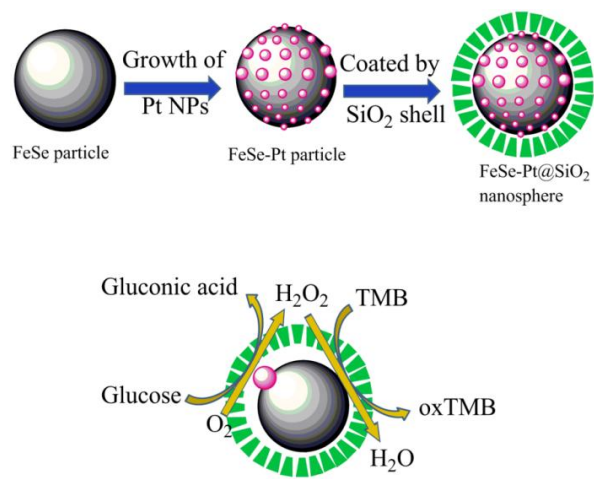
For glucose detection in real samples, different serum samples were collected for measuring the amount of glucose. The sample was firstly centrifuged at 12 000 rpm for 10 min, and then the supernatant was diluted 10 times using acetate buffer (100 mM, pH 7.0), respectively. The glucose detection in serum samples was measured as described above. For specificity of the present method, 227 μ M lactose, 227 μ M Maltose, and 227 μ M fructose were used as control samples instead of glucose for the assay.

3 Results and Discussion

3.1. Characterization

The FeSe-Pt@SiO₂ nanospheres were prepared by assembling multiple functional compartments attempting to tackle challenges in performing controlled encapsulated enzymatic catalysis. During the reaction process (as shown in scheme 1), firstly, the water dispersible FeSe particles were synthesized *via* a hydrothermal method. Secondly, FeSe-Pt particles with highly dispersed Pt NPs on the surfaces were prepared by reducing HPtCl₄ with NaBH₄ in the presence of FeSe particles. Finally, through a surfactant assembled sol-gel process with TEOS as the

SiO₂ source and cetyltrimethyl ammonium bromide (CTAB) as the structure directing agent, a meso structured SiO₂ layer was formed on the FeSe-Pt particles. The brown product FeSe-Pt@SiO₂ could be well dispersed in water. The resultant product was unambiguously analyzed by a series of characterizations.



Scheme 1 Schematic synthesis of the FeSe-Pt@SiO₂ Nanohybrids and mechanism of the enzymatic cascade reaction

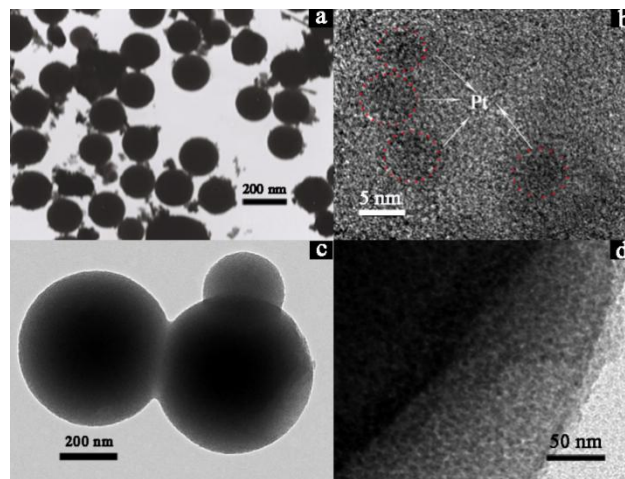


Fig. 1 (a) TEM image of FeSe particles. (b) High-resolution TEM image of FeSe-Pt particles. (c) TEM image and (d) HR-TEM of FeSe-Pt@SiO₂ microspheres

Fig. 1a shows typical transmission electron microscopy (TEM) images of the FeSe, in which FeSe were uniformly dispersed with a relatively narrow size distribution (150 \pm 10 nm) and a definite sphere structure. The close observation of a representative FeSe-Pt in Fig. 1b reveals surfaces of FeSe are evenly covered by ultrafine Pt NPs with the size of ca.7 nm. In view of the well dispersive Pt NPs on FeSe surfaces, we concluded that the FeSe could act as an efficient stabilizer or support in facilitating the dispersion and stability of Pt NPs, which would be beneficial to the following catalytic reaction. To stabilize these FeSe-Pt particles and keep their high enzyme-mimic activity during enzyme-catalyzed reactions, we intended to induce a SiO₂ layer on the surface of FeSe-Pt particles in our study. The obtained FeSe-Pt@SiO₂ microspheres (Fig. 1c) exhibit a more regular spherical shape with smooth surfaces due to the SiO₂ shells of the FeSe-Pt@SiO₂ microspheres, compared with FeSe particles.

Figure 1d shows a HRTEM image taken from the FeSe-Pt@SiO₂ microspheres, which indicates that the thickness of SiO₂ layer was about 100 nm.

Fig. 2a shows the FTIR spectra of the FeSe-Pt nanospheres. The broad band in the region from 600 to 900 cm⁻¹ are associated with the Fe-Se stretching⁴³. The bands 2900 cm⁻¹ are ascribed to the C-H vibrating and O-H vibrating, respectively⁴⁰.

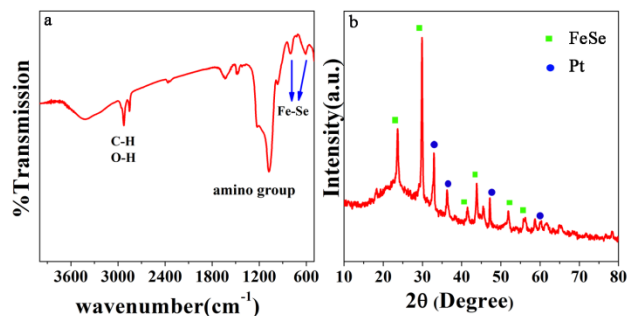


Fig. 2 (a) The FT-IR spectrum and (b) the wide angle XRD patterns of the FeSe-Pt nanospheres

Typical bands assigned to amino group are visible at 1650 to 1590 cm⁻¹ and 1038 cm⁻¹¹²⁸. This FT-IR spectrum indicates that FeSe particles are capped with amino groups. The absence of XRD peaks originating from iron species and Pt (Fig. 2b). These XRD peaks can be well indexed with the signatures of FeSe (JCPDS no. 65-1876) and Pt (JCPDS no. 04-0802). In case of Pt loading, it was seen that the crystal phase of FeSe did not change after hybridization with Pt, suggesting a strong interaction between FeSe and Pt. Moreover, no other impurity phase was seen, indicating the FeSe-Pt to be a two-phase composite.

3.2 Kinetics investigations of peroxidase-like catalysis activities of FeSe-Pt@SiO₂ nanospheres

In our study, we proved that FeSe-Pt@SiO₂ nanospheres possessed both intrinsic GOx- and peroxidase-mimic activities, and engineered an artificial enzymatic cascade system with high activity and stability based on this nanostructure. H₂O₂ is the main product of the glucose oxidase (GOx)-catalyzed reaction. Therefore, a self-organized cascade reaction could be realized using FeSe-Pt@SiO₂ nanospheres only. The proposed principle for the artificial enzymatic cascade system is described as follows (scheme 1).

The process was performed by a tandem catalysis starting from the oxidation of the glucose in the presence of O₂ catalyzed by the Pt NPs on the surface of FeSe particles in the FeSe-Pt@SiO₂ nanospheres, yielding gluconic acid and H₂O₂. Subsequently, H₂O₂, as the only harmful product of the reaction, was directly catalyzed by FeSe to oxidize TMB, producing H₂O and the oxidation of TMB (oxTMB) with blue color.

The peroxidase-like activity of the FeSe-Pt@SiO₂ nanospheres was evaluated by the catalytic oxidation of peroxidase substrate TMB in the presence of H₂O₂ through the time-dependent absorbance changes at 652 nm (characteristic absorbance originated from the oxidation of TMB). As shown in Fig. 3, in the absence of the FeSe-Pt@SiO₂ nanospheres, the solution containing TMB and H₂O₂ (the curve a) and the solution containing TMB and glucose (the curve b) display no absorption

in the maximum absorbance at 652 nm. This indicates that H₂O₂ and glucose can not catalyze the oxidation of TMB without catalyst. Additionally, in the absence of H₂O₂ and glucose, while presence of FeSe-Pt@SiO₂ nanospheres (the curve c), little or almost no absorption changes was observed in the (FeSe-Pt@SiO₂ nanospheres + TMB) system. More importantly, in the presence of H₂O₂, the resulting FeSe-Pt@SiO₂ nanospheres could show much higher catalysis activity in terms of the rate of absorbance changes at 652 nm (the system d). On the micro level, on one hand, the Pt NPs dispersed on the surface of FeSe could donate electrons to reduce H₂O₂ via the electron transfer. On the other hand, FeSe semiconductor could also donate electrons to reduce H₂O₂ via the electron transfer. Again, the use of FeSe “support” could significantly improve the dispersion and stability of the Pt to allow for better distribution. Take the above into consideration, these results may in turn facilitate greatly enhanced peroxidase-like catalysis activities of FeSe-Pt@SiO₂ nanospheres.

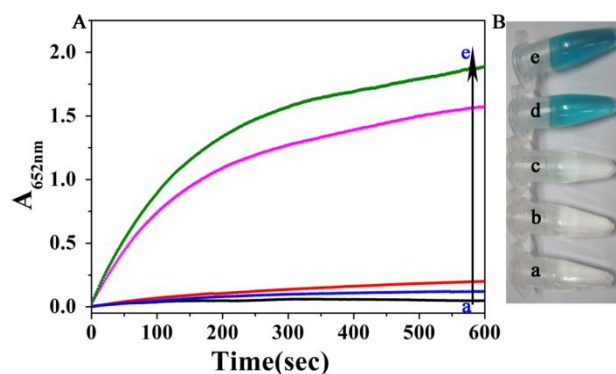
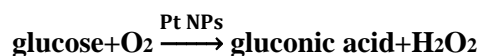


Fig. 3 The peroxidase-like activity in different systems under the reaction conditions of 115 μM TMB, 2.0 mM H₂O₂, 2.0 mM glucose, and a catalyst concentration of 30 μg mL⁻¹ in 100 mM acetate buffer (pH 4.0) at room temperature. (a) TMB+H₂O₂; (b) TMB+glucose; (c) TMB+FeSe-Pt@SiO₂ nanospheres; (d) TMB+ FeSe-Pt@SiO₂ nanospheres +H₂O₂; (e) TMB+ FeSe-Pt@SiO₂ nanospheres +glucose.

We first evaluated the GOx-mimicking activity of FeSe-Pt@SiO₂ nanospheres in solution and studied the mechanism of this reaction occurring at the nanoscale surface. FeSe-Pt@SiO₂ nanospheres prepared were incubated with glucose at room temperature for 30 min. When TMB was added to the solution, we found that the color of the solution turned blue, with a characteristic absorbance peak at 652 nm (the system d). The catalytic reaction is shown as the following equation: (1)



3.3 Optimization of experimental conditions

It is evident from Fig. 4a that free FeSe and Pt had little GOx-mimicking catalytic activity, while the hybrid catalyst exhibited surprisingly high activity, a factor of 10-16 fold excess higher than that of FeSe (15.6 ± 0.4%) and Pt (10.5 ± 0.4%) alone at the same concentration, suggesting synergistic coupling effects between the two poorly-active components in the composite for GOx-mimicking. In a control experiment, it was found that the physical mixture of FeSe and Pt (FeSe & Pt) presented much lower activity (12 ± 2%) than the composite (FeSe-Pt), indicating the importance of *in situ* reduction of Pt NPs on FeSe to initiate

the high-performance catalysis. This further highlighting that the chemical coupling between the two components was necessary to improve the activity. Furthermore, one observed that the catalytic activity increased with increasing FeSe-Pt nanocomposite, time-dependent absorbance changes at 652 nm revealed the FeSe-Pt nanocomposite concentration dependent catalytic rate and activity (Fig. 4b).

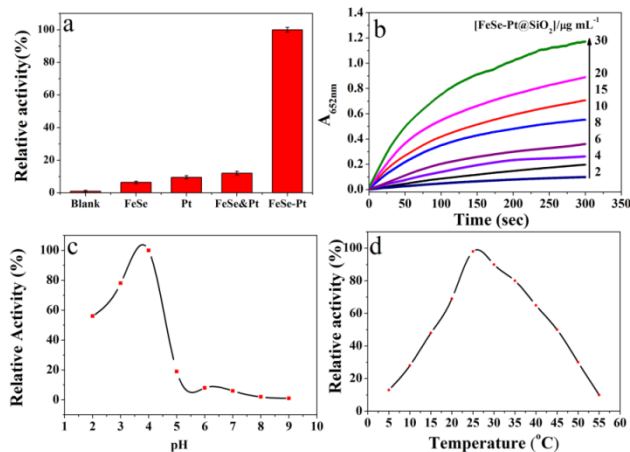


Fig. 4 (a) Time-dependent absorbance changes at 652 nm in the presence of different concentrations of FeSe-Pt@SiO₂ nanospheres. (b) Comparison of the catalytic activities of FeSe, Pt-NPs, physical mixtures of FeSe, Pt NPs and the FeSe-Pt hybrid under the same conditions. Effects of pH (c), temperature (d) on catalytic activity of FeSe-Pt@SiO₂ nanospheres, respectively. The maximum point was set as 100%. Experiments were carried out in 100 mM acetate buffer (pH 4.0) containing 2.0 mM glucose and 115 μM TMB at 25 °C.

Similar to natural enzyme, the catalytic activity of FeSe-Pt nanocomposite was also dependent on pH (Fig. 4c) and temperature (Fig. 4d). To investigate the influence of pH and temperature on the properties of this artificial enzymatic cascade system, 100 mM acetate buffer solution from pH 2.0 to 9.0 and temperature from 5 °C to 55 °C was used for current measurement. The velocity of the cascade reaction was the highest at pH 4.0 and 25 °C. In order to verify the synergistic effect in the hybrid, the pH and temperature were fixed at 4.0 and 25 °C, respectively.

To gain further insight into the discrepancy in mechanism of GOx-mimicking catalytic activity of the FeSe-Pt@SiO₂ nanospheres, the steady-state kinetic assays were carried out by changing one substrate concentration in a certain range while keeping the other substrate concentration constant. The steady-state kinetic parameters (K_m and V_{max}) from the initial reaction rate were calculated using Lineweaver-Burk plots of the double reciprocal of the Michaelis-Menten equation $1/v = (K_m/V_{max}) \cdot (1/[S]) + 1/V_{max}$, where v is the initial velocity, $[S]$ is the concentration of substrate, V_{max} represents the maximal reaction velocity, K_m signifies the Michaelis constant. As listed in Table 1, the apparent K_m value of the FeSe-Pt@SiO₂ nanospheres with glucose as substrate under the optimum conditions was two times lower than that of GOx, suggesting that the FeSe-Pt@SiO₂ nanospheres had a larger affinity for glucose than GOx, presumably resulting from its FeSe-Pt carriers with strong adsorption to glucose.

Table 1. Comparison of the Kinetic Parameters between FeSe-Pt@SiO₂ and GOx

Catalyst	Substance	K_m [mM]	V_{max} [10 ⁻³ s ⁻¹]	Reference
FeSe-Pt@SiO ₂	glucose	2.45	5.1	this work
GOx	glucose	4.87	2.85	⁴⁴

Additionally, the V_{max} of the FeSe-Pt@SiO₂ nanospheres with glucose as the substrate is two times larger than that of glucose, which is in favor of a higher reaction rate. This might be attributed to the presence of small Pt NPs on the surface of a FeSe as well as the electron transfer capability of the FeSe itself.

3.4 Bioassay

Given the intrinsic peroxidase properties of FeSe-Pt@SiO₂ nanospheres, a colorimetric method for detection of H₂O₂ using the FeSe-Pt@SiO₂ nanospheres catalyzed blue color reaction has been established. As shown in Fig. 5a, the typical UV-vis absorbance intensity at $\lambda = 652$ nm vs. H₂O₂ concentration indicates that more H₂O₂ introduced the stronger absorption peak intensity, which results in the corresponding calibration plot shown in Fig. 5c. The linear detection range is from 2.27 nM to 1.14 mM ($R^2 = 0.97$). The detection limit is estimated to be 0.227 nM.

To investigate the glucose-responsive capacity of this artificial enzymatic cascade system, different amounts of glucose were added to the test buffer on the basis of the optimal experimental conditions. As can be seen in Fig. 5b, the absorbance at 652 nm of oxidized TMB increased gradually with the increasing glucose concentrations. The glucose response curve and the corresponding calibration plot is described in Fig. 5d. The linear range for glucose was 11.36 nM to 227 μM with the limit of detection of 1.136 nM, revealing the FeSe-Pt@SiO₂ nanospheres are superior in sensitivity to previously reported peroxidase mimetics, the results were shown in Table 2.

based on Fe₃O₄ nanoparticles (30 μM) and Carbon 75 nanoparticles (20 μM).

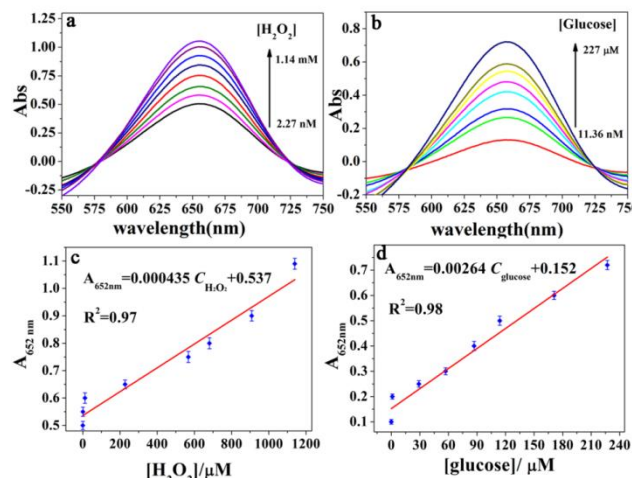


Fig. 5 Typical UV-vis absorption spectra obtained for detection of (a) H₂O₂ and (b) glucose based on the artificial enzymatic cascade system using FeSe-Pt@SiO₂ nanospheres under the optimized conditions. (c) typical dose-response curve for H₂O₂ detection; (d) typical dose-response curve for glucose detection.

Table 2. Comparison of performances of proposal mimetic enzyme for glucose detection with those of other mimetic enzymes based on differential materials

Mimetic enzyme	Linear range (μM)	Limit of detection (nM)
FeSe-Pt@SiO ₂	0.01136-227	1.136
⁴⁵ GO-Fe ₃ O ₄	2-200	240
⁴⁶ Carbon nanoparticles	0.05-1	2.0×10^4
⁴⁰ Fe ₃ O ₄	50-1000	3.0×10^4
⁴⁷ g-C ₃ N ₄	1-10	1.0×10^3
⁴⁸ BiOBr microspheres	2-40	800

Responsive specificity is also one important aspect of this artificial enzymatic cascade system. It is well known that GOx possesses a very high specificity toward glucose comparing with any other sugars. Experiments with interferences including 227 μM glucose analogues were conducted to test the selectivity of the the glucose analogues. Fig. 6a exhibits that as high as 227 μM control samples were investigated, however, no detectable current variation signal was observed under the same test condition.

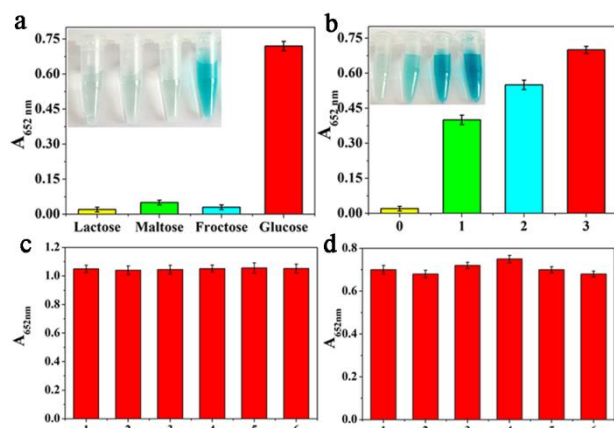


Fig. 6 (a) Selectivity analysis for glucose response. Inset: corresponding photographs of the colored reaction mixtures; (b) The glucose concentration for blank (0) and diluted serum samples (1-3); Inset: corresponding photographs of the colored reaction mixtures. The reproducibility of the developed enzyme mimic sensor for detecting (c) H₂O₂ and (d) glucose.

It is consistent with the high specificity of GOx for glucose. The results indicate that the as-proposed FeSe-Pt@SiO₂ nanospheres can be applied for constructing robust glucose-responsive devices. The proposed method was applied to detect glucose in different serum samples and the results are shown in Fig. 6b. According to the linear calibration curve mentioned above, glucose in the sample can be calculated as 0 mM, 2.82 mM, 4.52 mM and 6.23 mM, respectively. The general range of blood glucose concentration in healthy and diabetic persons is about 3-8mM and 9-40 mM, respectively^{46, 49}. Therefore, the proposed method could be applied to detect glucose in real samples. The reproducibility of the enzyme mimic sensor was investigated by analysis of H₂O₂ and glucose in the concentration of 1.14 mM and 227 μM , respectively, with six repeatedly prepared FeSe-Pt@SiO₂ nanospheres. The results were shown in Fig. 6c and 6d. The equal sensors displayed similar absorbance responses. It revealed that the enzyme mimic sensor for H₂O₂ and glucose

detection exhibited satisfied fabrication reproducibility. Moreover, after the storage for one week, it remained 95.9% of the initial catalytic activity, which revealed the sensing format possessed acceptable storage stability.

4 Conclusion

In summary, through a simple three-step assembly method, FeSe-Pt@SiO₂ nanospheres nanoreactor was synthesized. The results indicated that the prepared FeSe-Pt@SiO₂ nanospheres possessed both intrinsic glucose oxidase (GOx-) and peroxidase-mimic activities, the FeSe-Pt@SiO₂ nanospheres as robust nanoreactors can catalyze a self-organized cascade reaction, which includes oxidation of glucose by oxygen to yield gluconic acid and H₂O₂, and then oxidation of 3,3',5,5'-tetramethylbenzidine (TMB) by H₂O₂ to produce a colour change. Based on this, a simple, cheap, and highly selective and sensitive colorimetric method to detect glucose in serum samples was developed. We expected that FeSe-Pt@SiO₂ nanospheres cascade catalysis would have potential applications in biotechnology and clinical diagnosis field.

Acknowledgements

This work was supported by the National Natural Science Foundation of China (No. 21375079, 21105056) and Project of Development of Science and Technology of Shandong Province, China (No. 2013GZX20109)

Notes and references

College of Chemistry and Material Science, Shandong Agricultural University, Taian, Shandong 271018, P.R. China. Fax: +86 538 8242251; Tel: +86 538 8247660; E-mail: ashy@sdau.edu.cn (S.Y. Ai)

- P. A. Srere, *Annu. Rev. Biochem.*, 1987, **56**, 89-124.
- R. N. Perham, *Annu. Rev. Biochem.*, 2000, **69**, 961-1004.
- X. Huang, H. M. Holden and F. M. Raushel, *Annu. Rev. Biochem.*, 2001, **70**, 149-180.
- C. M. Agapakis, P. M. Boyle and P. A. Silver, *Nat. Chem. Biol.*, 2012, **8**, 527-535.
- C. Grondal, M. Jeanty and D. Enders, *Nat Chem*, 2010, **2**, 167-178.
- K. C. Nicolaou and J. S. Chen, *Chem. Soc. Rev.*, 2009, **38**, 2993-3009.
- C. Zhao and J. A. Lercher, *Angew. Chem. Int. Ed.*, 2012, **51**, 5765-5765.
- Y. Song, K. Qu, C. Zhao, J. Ren and X. Qu, *Adv. Mater.*, 2010, **22**, 2206-2210.
- M. I. Kim, Y. Ye, B. Y. Won, S. Shin, J. Lee and H. G. Park, *Adv. Funct. Mater.*, 2011, **21**, 2868-2875.
- X.-X. Wang, Q. Wu, Z. Shan and Q.-M. Huang, *Biosens. Bioelectron.*, 2011, **26**, 3614-3619.
- Y. Jv, B. Li and R. Cao, *Chem. Commun.*, 2010, **46**, 8017-8019.
- R. Chandrawati and F. Caruso, *Langmuir*, 2012, **28**, 13798-13807.
- M. T. Reetz, *J. Am. Chem. Soc.*, 2013, **135**, 12480-12496.
- N. T. S. Phan, C. S. Gill, J. V. Nguyen, Z. J. Zhang and C. W. Jones, *Angew. Chem. Int. Ed.*, 2006, **45**, 2209-2212.
- J. Shimada, T. Maruyama, M. Kitaoka, H. Yoshinaga, K. Nakano, N. Kamiya and M. Goto, *Chem. Commun.*, 2012, **48**, 6226-6228.

16. A. Grotzky, T. Nauser, H. Erdogan, A. D. Schlüter and P. Walde, *J. Am. Chem. Soc.*, 2012, **134**, 11392-11395.
17. R. J. R. W. Peters, M. Marguet, S. Marais, M. W. Fraaije, J. C. M. van Hest and S. Lecommandoux, *Angew. Chem. Int. Ed.*, 2014, **53**, 146-150.
18. M. Filice, M. Marciello, M. d. P. Morales and J. M. Palomo, *Chem. Commun.*, 2013, **49**, 6876-6878.
19. J. Liu, S. Z. Qiao, J. S. Chen, X. W. Lou, X. Xing and G. Q. Lu, *Chem. Commun.*, 2011, **47**, 12578-12591.
20. Z. Wu, K. Yu, S. Zhang and Y. Xie, *J. Phys. Chem. C*, 2008, **112**, 11307-11313.
21. Z. Chen, Z.-M. Cui, F. Niu, L. Jiang and W.-G. Song, *Chem. Commun.*, 2010, **46**, 6524-6526.
22. J. C. Park, J. U. Bang, J. Lee, C. H. Ko and H. Song, *J. Mater. Chem.*, 2010, **20**, 1239-1246.
23. X. Fang, Z. Liu, M.-F. Hsieh, M. Chen, P. Liu, C. Chen and N. Zheng, *ACS Nano*, 2012, **6**, 4434-4444.
24. S. Wang, M. Zhang and W. Zhang, *ACS Catalysis*, 2011, **1**, 207-211.
25. T. Harada, S. Ikeda, F. Hashimoto, T. Sakata, K. Ikeue, T. Torimoto and M. Matsumura, *Langmuir*, 2010, **26**, 17720-17725.
26. L. Chen, B. Sun, X. Wang, F. Qiao and S. Ai, *J. Mater. Chem. B*, 2013, **1**, 2268-2274.
27. Y. Jv, B. Li and R. Cao, *Chem. Commun.*, 2010, **46**, 8017-8019.
28. X. Wang, X. Chen, A. Thomas, X. Fu and M. Antonietti, *Adv. Mater.*, 2009, **21**, 1609-1612.
29. E. H. Boymans, P. T. Witte and D. Vogt, *Catal. Sci. Technol.*, 2015, **5**, 176-183.
30. C. Liu, C. F. Bender, X. Han and R. A. Widenhoefer, *Chem. Commun.*, 2007, 3607-3618.
31. H. Wang, S. Li, Y. Si, Z. Sun, S. Li and Y. Lin, *J. Mater. Chem. B*, 2014, **2**, 4442-4448.
32. H. Jiang, Z. Chen, H. Cao and Y. Huang, *Analyst*, 2012, **137**, 5560-5564.
33. X. Chen, J. Zhang, X. Fu, M. Antonietti and X. Wang, *J. Am. Chem. Soc.*, 2009, **131**, 11658-11659.
34. Y. Zhang, C. Xu, B. Li and Y. Li, *Biosens. Bioelectron.*, 2013, **43**, 205-210.
35. C. Sun, X. Chen, J. Xu, M. Wei, J. Wang, X. Mi, X. Wang, Y. Wu and Y. Liu, *J. Mater. Chem. A*, 2013, **1**, 4699-4705.
36. B. Sreedhar, P. S. Reddy and D. K. Devi, *The Journal of Organic Chemistry*, 2009, **74**, 8806-8809.
37. J. M. Perez, F. J. Simeone, A. Tsourkas, L. Josephson and R. Weissleder, *Nano Lett.*, 2004, **4**, 119-122.
38. O. Bomat íMiguel, M. P. Morales, P. Tartaj, J. Ruiz-Cabello, P. Bonville, M. Santos, X. Zhao and S. Veintemillas-Verdaguer, *Biomaterials*, 2005, **26**, 5695-5703.
39. Y.-S. Chang, S. Savitha, S. Sadhasivam, C.-K. Hsu and F.-H. Lin, *J. Colloid Interface Sci.*, 2011, **363**, 314-319.
40. H. Wei and E. Wang, *Anal. Chem.*, 2008, **80**, 2250-2254.
41. X. Qian, D. Xiong, A. M. Asiri, S. B. Khan, M. M. Rahman, H. Xu and D. Zhao, *J. Mater. Chem. A*, 2013, **1**, 7525-7532.
42. L. Han, Y. Lv, A. M. Asiri, A. O. Al-Youbi, B. Tu and D. Zhao, *J. Mater. Chem.*, 2012, **22**, 7274-7279.
43. D. S. Han, B. Batchelor and A. Abdel-Wahab, *Environ. Prog. Sustain. Energy*, 2013, **32**, 84-93.
44. M. Liu, H. Zhao, S. Chen, H. Yu and X. Quan, *Chem Commun*, 2012, **48**, 7055-7057.
45. Y.-l. Dong, H.-g. Zhang, Z. U. Rahman, L. Su, X.-j. Chen, J. Hu and X.-g. Chen, *Nanoscale*, 2012, **4**, 3969-3976.
46. W. Shi, Q. Wang, Y. Long, Z. Cheng, S. Chen, H. Zheng and Y. Huang, *Chem. Commun.*, 2011, **47**, 6695-6697.
47. T. Lin, L. Zhong, J. Wang, L. Guo, H. Wu, Q. Guo, F. Fu and G. Chen, *Biosens. Bioelectron.*, 2014, **59**, 89-93.
48. L. Li, L. Ai, C. Zhang and J. Jiang, *Nanoscale*, 2014, **6**, 4627-4634.
49. Y. Song, K. Qu, C. Zhao, J. Ren and X. Qu, *Adv. Mater.*, 2010, **22**, 2206-2210.